RESEARCH ARTICLE

Optimized immobilization strategy for dirhodium (II) carboxylate catalysts for C–H functionalization and their implementation in a packed bed flow reactor

Taylor A. Hatridge,[+[a]] Wenbin Liu,[+[b]] Chun-Jae Yoo,[+[a]] Huw M. L. Davies,*[[b]] Christopher W. Jones*[[a]]

[a] Ms. Taylor A. Hatridge, Dr. Chun-Jae Yoo, Prof. Dr. Christopher W. Jones
School of Chemical & Biomolecular Engineering
Georgia Institute of Technology
311 Ferst Dr, Atlanta, GA 30332, USA
E-mail: cjones@chbe.gatech.edu

[b] Dr. Wenbin Liu, Prof. Dr. Huw M. L. Davies
Department of Chemistry
Emory University
1515 Dickey Drive, Atlanta, GA 30322, USA
E-mail: hmdavie@emory.edu

[+]These authors contributed equally to this work.
Supporting information for this article is given via a link at the end of the document.

Abstract: Herein we demonstrate a packed bed flow reactor capable of achieving highly regio- and stereoselective C–H functionalization reactions using a newly developed Rh_2(*S*-2-Cl-5-CF_3TPCP)$_4$ catalyst. To optimize the immobilized dirhodium catalyst employed in the flow reactor, we systematically study both (i) the effects of ligand immobilization position, demonstrating the critical factor that the catalyst-support attachment location can have on the catalyst performance, and (ii) silica support mesopore length, demonstrating that decreasing diffusional limitations leads to increased accessibility of the active site and higher catalyst turnover frequency. We employ the immobilized dirhodium catalyst in a simple packed bed flow reactor achieving comparable yields and levels of enantioselectivity to the homogeneous catalyst employed in batch and maintain this performance over ten catalyst recycles.

Introduction

The use of noble metal catalysts to achieve selective C–H functionalization reactions has enabled the development of numerous new synthetic methodologies, unlocking novel routes for total synthesis.[1] In particular, the use of dirhodium catalysts and diazo compounds has led to the ability to achieve highly regio- and stereoselective reactions accessed through metal carbene intermediates.[2] The application of this rhodium carbene chemistry to the pharmaceutical industry could help transform the large-scale manufacture of medicinal drugs. Because conventional organic synthesis of biologically active molecules requires many steps and subsequent purifications, drug synthesis often generates extensive amounts of waste and results in a relatively low yield of the respective target molecules.[3] Thus, there is both environmental and economic pressure to implement more efficient methods to achieve the synthesis of pharmaceutical compounds via innovative engineering and chemistry solutions.

Despite the promise of dirhodium catalyzed C–H functionalization as an alternate methodology, certain obstacles have prevented widespread industrial acceptance of rhodium carbene mediated C–H functionalization. For example, a key challenge is the safety concern associated with handling large quantities of toxic, unstable diazo compounds at the manufacturing site;[4] however, strategic execution of flow chemistry may allow the upstream synthesis of diazo compounds and their immediate downstream consumption.[5,6] Another barrier for industrial implementation is the high cost of the noble metal and ligands, as well as the intricate synthesis of the dirhodium tetracarboxylate catalyst complex (Rh_2L_4). This challenge is best mitigated by maximizing the total turnover number (TON) of the dirhodium catalyst, which can be achieved via a range of techniques to prolong the catalyst lifetime, including: catalyst design and optimization, increasing the catalyst turnover frequency (TOF), or decreasing the rate of catalyst deactivation.[7] Additionally, if catalyst deactivation rates are not too significant, catalyst TON can be elevated by catalyst recycle, which can be facilitated by the development of heterogeneous catalysts[8] that are amenable to deployment in flow reactors. Thus, various groups have studied the immobilization of molecular catalysts based on numerous chiral ligand scaffolds.[9] Davies et al. immobilized an array of chiral dirhodium catalysts on a pyridine functionalized, crosslinked resin; however, the noncovalent coordination between pyridine and rhodium may result in catalyst leaching during reaction.[10] As an alternative immobilization technique, Takeda et al. modified a chiral ligand of several dirhodium catalysts that were then copolymerized with styrene and a flexible crosslinker to provide polymeric catalyst materials that offered relatively stable catalytic activity over multiple recycles.[11] Our group previously designed and synthesized a polymer/silica composite hollow fiber reactor, in which the embedded silica particles were functionalized with immobilized dirhodium carboxylate catalysts, including (*p*-dodecylphenyl-sulfonyl)prolinato (DOSP) and (4-bromophenyl)-2,2-diphenyl-cyclopropanecarboxylato (*p*-BrTPCP) ligands.[6b,12] However, the use of the unusual polymeric hollow fiber reactor and the limited knowledge of the impact of different immobilization strategies for the target carboxylate ligands are two aspects of our

prior work that could limit rapid deployment of C–H functionalization in a practical flow process.

In recent years, Davies and coworkers have achieved the C–H functionalization of unactivated C–H bonds using the sterically hindered dirhodium tetrakis(1,2,2-triarylcyclopropane carboxylate) catalysts, $Rh_2(TPCP)_4$. With substituents at different positions of the C1-aryl rings, $Rh_2(TPCP)_4$ adopted defined high-symmetry conformations and was capable of catalyzing highly site- and stereoselective C–H functionalization reactions. Modifying the identity and location of functional groups on the aryl rings altered the symmetry and selectivity of the $Rh_2(TPCP)_4$ catalyst,[13] which has inspired us to conduct a systematic exploration on the effect of the location of linker installation for catalyst immobilization in the *ortho*-Cl $Rh_2(TPCP)_4$ catalysts. In this work, we evaluate the effect of ligand immobilization position and employ a conventional, rapidly deployable fixed bed flow reactor using a newly developed dirhodium catalyst, Rh_2(*S*-2-Cl-5-CF_3TPCP)$_4$, supported on porous silica powders for selective functionalization of unactivated secondary (C2) sp^3 C–H bonds.

Results and Discussion

Optimizing Immobilization Position

When considering the appropriate immobilization strategy for any chiral catalyst, one must account for the catalyst's inherent symmetry and the nature of the catalyst's binding site so as to preserve its intrinsic performance. For the class of $Rh_2(TPCP)_4$ catalysts containing a triarylcyclopropane scaffold, the linker could potentially be installed on any of the three phenyl rings; however, these aryl rings are critical components of the catalyst's chiral pocket. To rigorously study the effect of linker location on each of these rings, we chose Rh_2(*S*-*o*-ClTPCP)$_4$ as our model catalyst, as its unique C_4 symmetric configuration consists of the three aryl rings oriented in three different directions (as shown in **Figure 1**).[13b] The C_1 *o*-Cl-aryl ring **A** points towards the active rhodium site of the catalyst and constitutes the chiral reaction pocket (top view); the C_2-phenyl ring **B**, which is *cis* to the *o*-Cl-aryl group, points to the equatorial side of the Rh–O disk and is furthest away from the Rh center (side view); while the other C_2-phenyl ring **C**, which is *trans* to the *o*-Cl-aryl group, is at the "closed" rhodium face, where four phenyl rings tilt toward each other and block the second potential active rhodium site (bottom view).

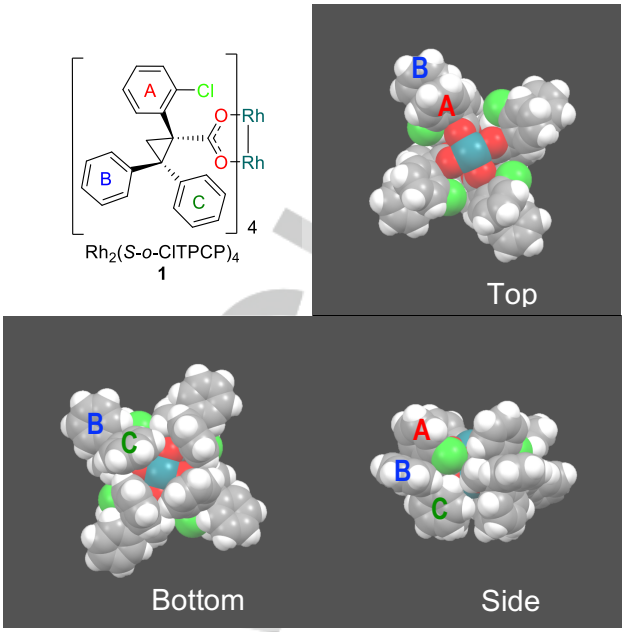

Figure 1. Chemical and crystal structures of Rh_2(*S*-*o*-ClTPCP)$_4$ catalyst (Teal: Rh, Red: O, Green: Cl, Grey: C, White: H). Aryl rings are labeled A, B, and C to show the possible locations for the introduction of a covalently bound linker to tether the catalyst to a heterogeneous silica support.

Therefore, we hypothesized that the installation of the linker would be preferred on either ring **B** or **C**, as placement on ring **A** might interfere with the active site and attenuate the catalyst's activity and selectivity. To test this hypothesis, we synthesized three Rh_2(*S*-*o*-ClTPCP)$_4$ derivatives with an ethynyl substituent on rings **A**, **B**, and **C**, respectively. The synthesis of the complexes involved a six-step sequence (**Figure 2**, see Supporting Information for detailed synthesis). The first step is a rhodium-catalyzed asymmetric cyclopropanation of an aryldiazoacetate with the 1,1-diarylethylene. The derivative **8a** was generated using the symmetric 1,1-diphenylethylene, while the other two derivatives (**8b** and **8c**) were obtained as diastereomers using 1-phenyl,1'-(*p*-bromophenyl)ethylene. The TIPS-protected ethynyl group was then installed by a palladium-catalyzed Sonogashira coupling, followed by hydrolysis to reveal the desired carboxylic acid ligand. Then, a controlled mono-ligand exchange, followed by deprotection gave the Rh_2(*S*-*o*-ClTPCP)$_4$ derivative with terminal ethynyl group at the desired location (**9a-c**). Further modification *via* copper-catalyzed [3+2] alkyne–azide cycloaddition creates two families of modified catalysts: an analogous homogeneous catalyst linked to a "dummy" silane (**2a**, **2b**, **2c**, **Figure 2**) and a heterogeneous catalyst linked to a solid silica support (Syloid®, Grace) (**3a**, **3b**, **3c**, **Figure 2**).

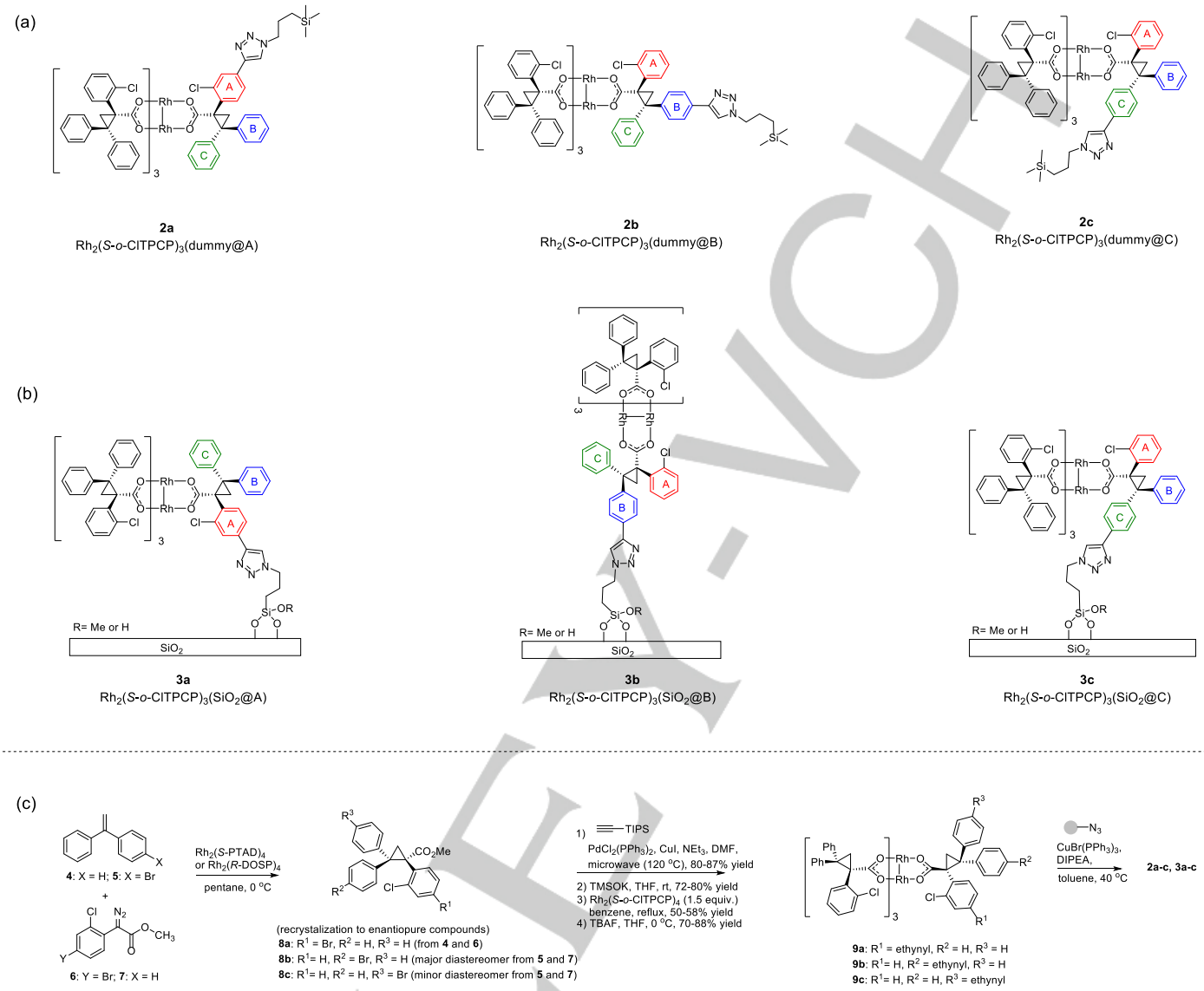

Figure 2. The synthesized homogeneous Rh_2(*S*-*o*-ClTPCP)$_4$ derivative catalysts with a) dummy silane groups at A, B, and C positions, and b) the immobilized Rh_2(*S*-*o*-ClTPCP)$_4$ derivative catalysts via A, B, and C positions on a silica support

In this way, we were able to decouple the potential effects of the additional triazolepropyl trimethylsilane group covalently bound to the catalyst's chiral ligand and a possible steric hindrance between the catalytic active site and the silica support surface. The catalyst derivatives **2** and **3** were then subjected to a reference reaction between 4-bromopentylbenzene (**10**) and trifluoroethyl 4-bromophenyldiazoacetate (**11**). The substrate, **10**, has two possible C–H bonds that can be functionalized: the electronically favored benzylic C–H bond and the sterically favored terminal methylene (C2) C–H bond. Due to the sterically limited active site constructed by the four *o*-Cl-aryl rings in the Rh_2(*S*-*o*-ClTPCP)$_4$ catalyst, the C2 C–H bonds with less steric bulk are preferred, resulting in exceptionally high regioselectivity toward C2 C–H functionalization (91:9 rr, entry 1, **Figure 3**).[13e] The "dummy" silane-linked homogeneous catalysts (**2a**, **2b**, **2c**) all conducted the desired C–H functionalization in a stereoselective manner; however, the site selectivity and enantiomeric performance were slightly influenced by the ligand modification (**Figure 3**). Previous computational studies on the ortho-Cl-TPCP catalysts have revealed that this class of catalysts is quite rigid[13e] and consequently, the linker is reasonably well acommodated at all three positions; however, placing the linker at certain positions may alter the orientation of the chiral ligands and introduce steric hindrance at the catalytic active site. For catalyst **2a**, the placement of the "dummy" silane on ring **A** resulted in a yield (72%), regioselectivity (88:12), and enantiomeric excess (72%) that were markedly lower than those of the unmodified catalyst and the other derivatives **2b** and **2c**. Thus, we may conclude that the presence of a linker at position **A** affects the active site structure and may sterically hinder the substrate's approach to the reactive carbene, supporting our earlier hypothesis. Additionally, the heterogeneous silica-supported

catalysts (**3a**, **3b**, **3c**) showed similar reaction profiles to their homogeneous "dummy" linked counterparts (**2a**, **2b**, **2c**), demonstrating that changing the nature of the catalyst (from soluble to silica-supported) did not significantly impede its reactivity. However, the results confirmed that the location of the linker does affect catalyst performance. While the derivatives with linkers at rings **B** and **C** showed overall similar reactivity, placing the linker on ring **A** resulted in further decreased selectivity and yield. After immobilization on the silica surface, the active site of the catalyst **3a** would open toward the silica support (entry **d**, **Figure 2**), where the surface species might interact with the active site or hinder the substrate accessibility. Thus, we decided to move forward with the linker located on ring **B**, as its equatorial position is conserved in other catalyst geometries in the tetracarboxylate family, making it the optimal anchor site for all known TPCP-based dirhodium catalysts.[13, 14]

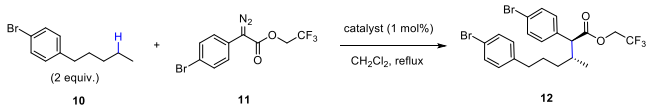

	Catalyst	Yield (%)[a]	rr (C2:Benzylic)	dr (C2)	ee (%)
1	Rh_2(*S*-*o*-ClTPCP)$_4$	87	91:9	96:4	77
2a	Rh_2(*S*-*o*-ClTPCP)$_3$(dummy@A)	72	88:12	95:5	72
2b	Rh_2(*S*-*o*-ClTPCP)$_3$(dummy@B)	83	93:7	94:6	77
2c	Rh_2(*S*-*o*-ClTPCP)$_3$(dummy@C)	80	91:9	95:5	77
3a	Rh_2(*S*-*o*-ClTPCP)$_3$(SiO_2@A)	69	85:15	94:6	65
3b	Rh_2(*S*-*o*-ClTPCP)$_3$(SiO_2@B)	83	90:10	95:5	76
3c	Rh_2(*S*-*o*-ClTPCP)$_3$(SiO_2@C)	78	92:8	95:5	79

[a] Indicates isolated yield

Figure 3. Investigation of the effect of immobilization location (**A**, **B**, or **C**) and catalyst nature (homogeneous as **2a-c** or immobilized on a silica support as **3a-c**) on Rh_2(*S*-*o*-ClTPCP)$_4$ catalyst activity and selectivity.

Tuning the Solid Silica Support

Next, we sought to modify the solid support as a means to probe whether active site accessibility affects the reactivity of the silica-supported Rh_2(*S*-*o*-ClTPCP)$_3$(ethynyl@B) catalysts. SBA-15 is a model, ordered mesoporous silica support material containing one dimensional cylindrical mesopores.[15] While the well-defined nature of the support material and uniform pore size and structure allows the synthesis of well-defined supported catalysts, the presence of long straight mesopores surrounding the active rhodium sites can lead to substrate or product transport limitations, depending on the reaction conditions and the diameter and length of the mesopores. Given that the dirhodium catalyzed C–H functionalization reactions are generally quite fast,[16] we postulated that transport through the channels could have a non-negligible effect on the overall reaction rate. Moreover, the decomposition of diazo compounds generates nitrogen gas, which may result in significant transport limitations in the porous support structure of our heterogeneous system. Thus, we hypothesized that shortening the pore length of the SBA-15 silica support would result in a faster diffusion of the reactants and products to and from the catalyst immobilized within the SBA-15 mesopores, while allowing the evolved nitrogen gas to more rapidly escape from the catalyst. To test this hypothesis, the Rh_2(*S*-*o*-Cl-TPCP)$_3$(ethynyl@B) catalyst was immobilized on regular SBA-15 (0.18 $mmol_{Rh2}$/g) and quasi-2D, platelet SBA-15 (0.20 $mmol_{Rh2}$/g) supports. The prepared regular and platelet SBA-15 supports have similar surface area (573 m^2/g vs 576 m^2/g), pore volume (1.3 cm^3/g vs 1.1 cm^3/g), and pore diameter (12 nm vs 13 nm); the only distinguishable difference is pore length, which can be verified by SEM and TEM images (**Figure 4**). While the regular SBA-15 has a straight or slightly bent rod-shaped structure (pore length >1 μm), the platelet SBA-15 has short (< 400 nm), straight pores.

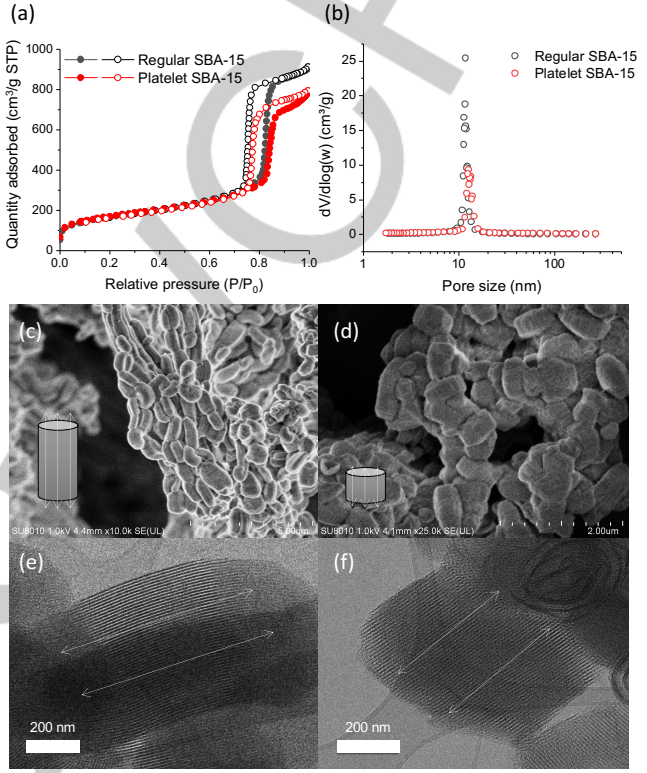

Figure 4. (a) Cryogenic nitrogen adsorption isotherms and (b) pore size distributions of regular and platelet SBA-15. SEM and TEM images of (c, e) regular SBA-15 (d, f) platelet SBA-15. The white lines represent pore directions.

The two SBA-15 immobilized catalysts were subjected to a batch cyclopropanation reaction between trichloroethyl diazoacetate and styrene, which was monitored via *in situ* FTIR. The rate of the dirhodium-catalyzed cyclopropanation reaction was evaluated based on the disappearance of the peak at 2100 cm^{-1}, which corresponds to the C=N_2 stretch of the diazo compound (**Figure 5**). The 0.13 M solution of **13** was consumed by the Rh_2(*S*-*o*-Cl-TPCP)$_4$ catalyst analogs at different rates: the homogeneous catalyst completed the reaction in 9 min, the catalyst immobilized on the quasi-2D support completed the reaction in 55 min, and the catalyst immobilized on the regular SBA-15 support completed the reaction in 125 min. The TOF of initial diazo consumption followed a similar trend. The homogenous Rh_2(*S*-*o*-Cl-TPCP)$_4$ catalyst gave a TOF of 45100 h^{-1}, which was noticeably faster than that of the immobilized catalysts, and the TOF for the platelet SBA-15 immobilized catalyst (13650 h^{-1}) was higher than that of the regular SBA-15 immobilized catalyst (7460 h^{-1}), demonstrating that shortening the support channels results in an increased reaction rate.

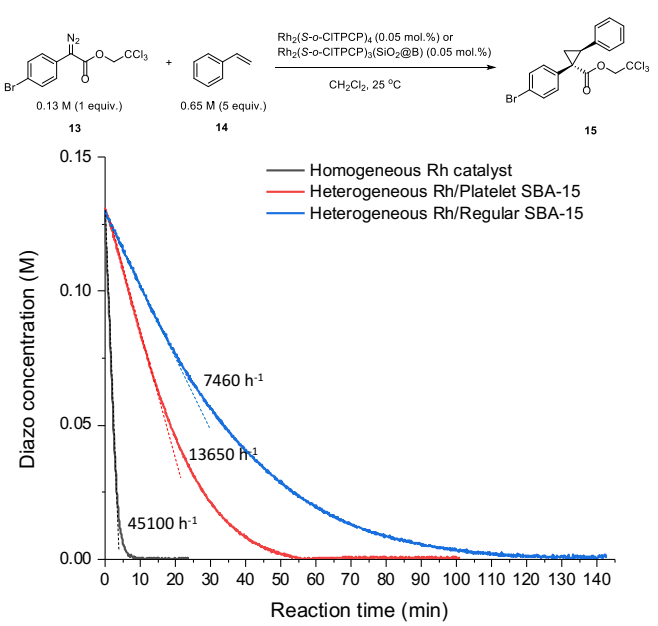

Figure 5. Effect of the length of mesopores in SBA-15 silica support on reaction time and catalyst TOF. Immobilization of the catalyst within a quasi-2D, platelet SBA-15 support mitigates some diffusional limitations of reactant and product to and from the dirhodium active site, increasing catalyst TOF.[18]

Development of Rh_2(S-2-Cl-5-CF_3TPCP)$_4$ Catalyst

After optimizing the catalyst immobilization position and silica support material, we sought to employ the optimal catalyst in the Rh_2(*S*-*o*-ClTPCP)$_4$ series in a packed bed flow reactor for C–H insertion of C2 C–H bonds. The Rh_2(*S*-2-Cl-5-BrTPCP)$_4$ catalyst (**16**) consistently gives enantio- and regioselectivities that outperform those of the Rh_2(*S*-*o*-ClTPCP)$_4$ catalyst.[13e] However, the installation of the ethynyl group, which is necessary for immobilization, requires a Sonogashira coupling with an aryl bromide leaving group. The presence of two aryl bromides on the Rh_2(*S*-2-Cl-5-BrTPCP)$_3$(Br@B) catalyst presents a selectivity issue that may result in a loss of control over the site of catalyst immobilization. Thus, we decided to develop a new Rh_2(*S*-2-Cl-5-BrTPCP)$_4$ analog with similar or better performance. To do so, the bromide moiety on the *o*-Cl-aryl ring would need to be replaced by a substituent with similar steric and electronic properties, but with no lability to Sonogashira coupling; hence, a trifluoromethyl group was proposed as a replacement functional group. The new Rh_2(*S*-2-Cl-5-CF_3TPCP)$_4$ catalyst (**17**) was synthesized (See Supporting Information for detailed synthesis) and subjected to the reference reaction with 1-bromo-4-pentylbenzene. The performance of the new catalyst was found to be comparable in site-, diastereo-, enantioselectivity, and yield to that of the Rh_2(*S*-2-Cl-5-BrTPCP)$_4$ catalyst (**Figure 6**). Thus, the Rh_2(*S*-2-Cl-5-CF_3TPCP)$_4$ was chosen as the optimal dirhodium catalyst for our flow reaction purposes and was subjected to immobilization on the platelet SBA-15 support via ring **B**.

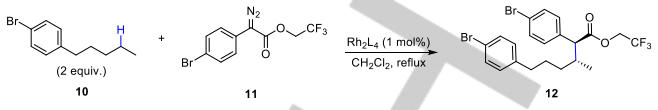

	Rh_2L_4	Yield (%)[a]	rr (C2:Benzylic)	dr (C2)	ee (%)
1	Rh_2(*S*-*o*-ClTPCP)$_4$	87	91:9	96:4	77
16	Rh_2(S-2-Cl-5-BrTPCP)$_4$	86	96:4	96:4	91
17	Rh_2(S-2-Cl-5-CF_3TPCP)$_4$	82	96:4	95:5	93

[a] Indicates isolated yield

Figure 6. Comparison of catalytic activity and selectivity between the Rh_2(*S*-2-Cl-5-BrTPCP)$_4$ and newly developed Rh_2(*S*-2-Cl-5-CF_3TPCP)$_4$ catalysts.

Implementation in Packed Bed Flow Reactor

Next, our optimized immobilized catalyst was implemented in flow. To mitigate pressure drop within the packed bed reactor and improve catalyst performance, the immobilized Rh_2(*S*-2-Cl-5-CF_3TPCP)$_3$(platelet SBA-15@B) was diluted with commercial silica (SiliaFlash P60). However, the abundance of silanols on the hydrophilic silica surface resulted in the introduction of O–H insertion reactions, which competed with the desired C–H functionalization. Therefore, we passivated the silanol groups with hexamethyldisilazane (HMDS) to create a hydrophobic silica surface that would attenuate O–H insertion reactions. The preparation of the packed bed and the flow system configuration are summarized in the Supporting Information.

The performance of the packed bed reactor, along with a comparison of performance to that of the homogeneous Rh_2(*S*-2-Cl-5-CF_3TPCP) catalyst employed in batch, are shown in **Figure 7.** With two exceptions (**20c**, **20d**), the C–H insertion products were synthesized with high yields (75-93%), as well as regio- and stereoselectivities (86-95% *ee*) commensurate with those obtained via the homogeneous/batch analog (**20a-b, 20e-i**). Although substrates **20c** and **20d** were obtained with lower yields (32% and 25%, respectively), a relatively high enantioselectivity (82% *ee*) was maintained in both reactions. These low yields are presumably caused by the slower rate of diazo decomposition due to the presence of the strongly electron-withdrawing nitro group (**20c**) and the coordination between the rhodium active site and the pyridine nitrogen (**20d**) for these two substrates. The similarity in performance between the heterogeneous catalyst implemented in the packed bed flow reactor and the homogeneous catalyst employed in batch supports our previous hypothesis that the immobilization via the equatorial ring **B** is robust and may be broadly applied to other Rh_2(TPCP)$_4$-derived catalysts. Additionally, the weight hourly space velocity (WHSV) of our system is large (570 hr^{-1} for substrates **20a-b, 20e-i**; 285 hr^{-1} for substrates **20c,d**) compared to some other reported supported catalysts for site- and enantioselective organic reactions.[17] This high WHSV and the low residence time (53 s for substrates **20a-b, 20e-i**; 106 s for substrates **20c,d**) show that our system has an efficient use of catalyst and may be capable of achieving high productivity to enable the scale-up of this system.

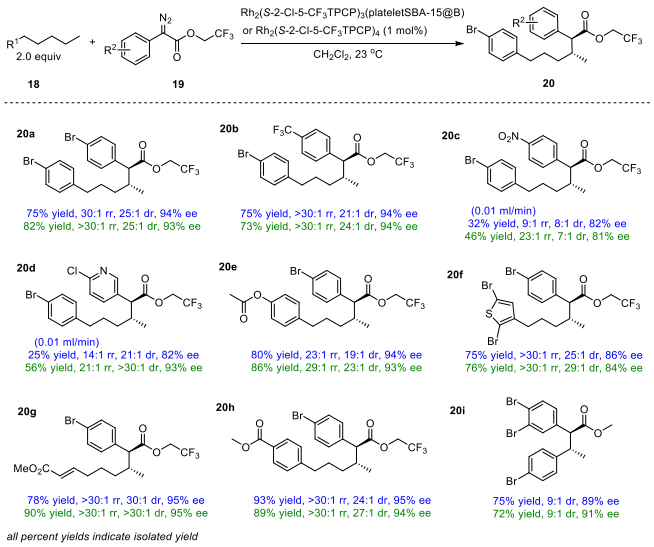

Figure 7. Substrate scope showing Rh_2(*S*-2-Cl-5-CF_3TPCP)$_4$ catalyst performance in flow (top, blue) and batch (bottom, green) reactions. The flow reactions were conducted at a flow rate of 0.02 mL/min, with the exception of substrates 20c and 20d, which were run at a flow rate of 0.01 mL/min to accommodate decreased reactivity.

One of the advantages of our catalyst immobilization strategy is that it enables the recycling of the dirhodium catalyst. To conduct our recyclability study, the same batch of catalyst was subjected to ten consecutive reactions without repacking the column between runs. As shown in Figure 8, the yields were consistent, with only a slight decrease from 75% to 67%, and the enantioselectivities were quite stable, decreasing only slightly from 93% to 89%. As we have previously shown,[4b] the rhodium catalyst is not prone to leaching from the silica support and the slight decrease in activity can be attributed to a slow deactivation of the catalyst over time.

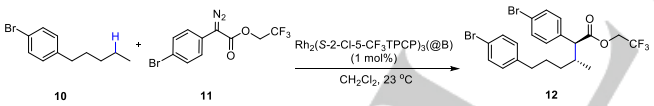

Recycle No.	1	2	3	4	5	6	7	8	9	10
Yield (%)[a]	75	76	76	75	78	73	71	70	68	67
rr	97:3	97:3	97:3	97:3	96:4	96:4	96:4	97:3	96:4	96:4
dr	96:4	96:4	96:4	96:4	96:4	96:4	96:4	96:4	96:4	96:4
ee (%)	94	90	90	90	89	90	89	90	90	89

[a] Indicates isolated yield

Figure 8. Recyclability results for the immobilized Rh_2(*S*-2-Cl-5-CF_3TPCP)$_3$(platelet SBA-15@B) catalyst. Yield and selectivity are largely maintained over the ten reaction cycles.

Conclusion

To optimize the immobilization of dirhodium tetracarboxylate catalysts, we systematically designed and synthesized an array of dirhodum catalysts with an inert linker covalently tethered to different aryl ring sites. The catalyst immobilized via the aryl ring at the equatorial position showed catalytic activity and selectivity most similar to those of the unmodified catalyst, as the linker location is removed from the vicinity of the active site. To increase the immobilized catalyst's TOF, the dirhodium carboxylate catalysts were immobilized on a quasi-2D, mesoporous platelet SBA-15 support via the equatorial aryl ring. Using this optimized immobilization strategy, the newly developed Rh_2(*S*-2-Cl-5-CF_3TPCP)$_4$ catalyst was deployed as a heterogeneous catalyst in a packed bed flow reactor to achieve enantioselective C–H functionalization reactions with similar reactivity and selectivity to the homogeneous catalyst utilized in batch. This catalytic performance was maintained over multiple recycles; therefore, we expect that this work may contribute to larger-scale synthesis of pharmaceutical compounds via the coupling of flow synthesis of diazo compounds[6] combined with flow synthesis using optimal immobilized dirhodium catalysts.

Acknowledgements

Financial support was provided by NSF under the CCI Center for Selective C−H Functionalization (CHE‐1700982). This material is based upon work supported by the National Science Foundation Graduate Research Fellowship Program under Grant No. DGE–1650044. Any opinions, findings, and conclusions or recommendations expressed in this material are those of the author(s) and do not necessarily reflect the views of the National Science Foundation.

Keywords: C–H activation • supported catalyst • carbene • mesoporous silica • diazonium compound

[1] a) K. Godula, D. Sames, *Science* **2006,** *312* (5770), 67-72; b) J. Wencel-Delord, F. Glorius, *Nat. Chem.* **2013,** *5* (5), 369-375; c) J. Yamaguchi, A. D. Yamaguchi, K. Itami, *Angew. Chem. Int. Ed.* **2012,** *51* (36), 8960-9009; d) D. A. Colby, R. G. Bergman, J. A. Ellman, *Chem Rev* **2010**, *110*, 624-655; e) D. A. Coby, A. S. Tsai, R. G. Bergman, J. A. Ellman, *Accounts of Chem. Res.* **2012**, *45*(6), 814-825; f) W. R. Gutekunst, P. S. Baran, *Chem. Soc. Rev.* **2011**, *40*(4), 1845-2040.

[2] a) M. P. Doyle, D. C. Forbes, *Chem. Rev.* **1998,** *98*, 911-936; b) M. P. Doyle, R. Duffy, M. Ratnikov, L. Zhou, *Chem. Rev.* **2010,** *110*, 704-724; c) A. Ford, H. Miel, A. Ring, C. N. Slattery, A. R. Maguire, M. A. McKervey, *Chem. Rev.* **2015,** *115*, 9981-10080.

[3] a) C. Jimenez-Gonzalez, D. J. Constable, C. S. Ponder, *Chem. Soc. Rev.* **2012,** *41* (4), 1485-1498; b) C. Jimenez-Gonzalez, C. S. Ponder, Q. B. Broxterman, J. B. Manley, *Org. Process Res. Dev.* **2011,** *15* (4), 912-917; c) R. A. Sheldon, *Green Chem.* **2007,** *9* (12) 1273–1283; d) L. Vaccaro, M. Curini, F. Ferlin, D. Lanari, A. Marrocchi, O. Piermatti, V. Trombettoni, *Pure Appl. Chem.* **2018,** *90* (1), 21-33.

[4] a) J. H. Simpson, A. S. Kotnis, R. P. Deshpande, D. J. Kacsur, J. Hamm, G. Kodersha, W. Merkl, D. Domina, S. Y. Wang in *Managing Hazardous Reactions and Compounds in Process Chemistry*, (Eds.: Pesti, J. A.; Abdel-Magid, A. F.), American Chemical Society: Washington DC, **2014**, pp. 235−244; b) S. P. Green, K. M. Wheelhouse, A. D. Payne, J. P. Hallet, P. W. Miller, J. A. Bull, *Org. Process Res. Dev.* **2020**, *24*(1), 67-84.

[5] a) T. Ye, M. A. McKervey, *Chem. Rev.* **1994**, *94*, 1091−1160; b) M. A. McKervey, *Chem. Rev.* **2015**, *115*, 9981−10080; c) S. T. R. Muller, A. Murat, D. Maillos, P. Lesimple, P. Hellier, T. Wirth, *Chem. Eur. J.* **2015**, *21*, 7016-7020; d) J. S. Poh, S. Makai, T. von Keutz, D. N. Tran, C. Battilocchio, P. Pasau, S. V. Ley, *Angew. Chem. Int. Ed.* **2015**, *54*, 7920-7923; e) N. M. Roda, D. N. Tran, C. Battilocchio, R. Labes, R. J. Ingham, J. M. Hawkins, S. V. Ley, *Org. Biomol. Chem.* **2015**, *13*, 2550-2554; f) D. N. Tran, C. Battilocchio, S. B. Lou, J. M. Hawkins, S. V. Ley, *Chem. Sci.* **2015**, *6*, 1120-1125; g) B. Pieber, C. O. Kappe, *Org. Lett.* **2016**, *18*, 1076-1079; h) K.A. Mix, M. R. Aronoff, R. T. Raines, *ACS Chem. Biol.* **2016**, *11*, 3233−3244; i) H. Wang, B. Martin, B. Schenkel, *Org. Process Res. Dev.* **2018**, *22*, 446-456; j) R. J. Sullivan, G. P. R. Freure, S. G. Newman, *ACS Catal.* **2019**, *9*, 5623-5630; k) E. M. D. Allouche, A. B. Charette, *Chem. Sci.*, **2019**, *10*, 3802-3806.

[6] a) D. Rackl, C. J. Yoo, C. W. Jones, H. M. L. Davies, *Org. Lett.* **2017,** *19* (12), 3055-3058; b) C. J. Yoo, D. Rackl, W. Liu, C. B. Hoyt, B. Pimentel, R. P. Liveley, H. M. L. Davies, C. W. Jones, *Angew. Chem. Int. Ed.* **2018,** *57* (34), 10923-10927.

[7] a) C. W. Jones *Top. Catal.* **2010,** *53* (13-14), 942-952; b) S. L. Scott *ACS Catal.* **2018**, *8*, 8597-8599.

[8] a) D. E. De Vos, M. Dams, B. F. Sels, P. A. Jacobs, *Chem. Rev.*, **2002**, *102*, 3615-3640 ; b) X. S. Zhao, X. Y. Bao, W. Guo, F. Y. Lee, *Mater. Today,* **2006**, *9*, 32-39; c) S. Shylesh, V. Schünemann, W. R. Thiel, *Angew. Chem. Int. Ed.*, **2010**, *49*(20), 3428-3459.

[9] a) C. E. Song, S. Lee, *Chem. Rev.* **2002**, 102, 3495−3524; b) A. Hu, H. L. Ngo, W. Lin, *J. Am. Chem. Soc.* 2003, 125, 38, 11490–11491; c) P. McMorn, G. J. Hutchings, *Chem. Soc. Rev.*, **2004**, *33*, 108-122; d) C. Li, *Catal. Rev.*, **2004**, *46*, 419-492 ; e) Q. H. Xia, H. Q. Ge, C. P. Ye, Z. M. Liu, K. X. Su, *Chem. Rev.*, **2005**, *105*(5), 1603–1662; f) A. Corma, H. Garcia, *Adv. Synth. Catal.*, **2006**, *348*, 1391–1412; g) M. Heitbaum, F. Glorius, I. Escher, *Angew. Chem. Int. Ed.*, **2006**, *45*(29), 4732-4762; h) J. M. Fraile, J. I. Garcia, J. A. Mayoral, *Chem. Rev.,* **2009**, *109*(2), 360–417.

[10] a) H. M. L. Davies, A. M. Walji, *Org. Lett.* **2003,** *5* (4), 479-482; b) H. M. L. Davies, A. M. Walji, *Org. Lett.* **2005,** *7* (14), 2941-2944; c) H. M. L. Davies, A. M. Walji, T. Nagashima, *J. Am. Chem. Soc.* **2004,** *126*, 4271-4280.

[11] a) K. Takeda, T. Oohara, M. Anada, H. Nambu, S. Hashimoto, *Angew. Chem. Int. Ed.* **2010,** *49* (39), 6979-6983; b) K. Takeda, T. Oohara, N. Shimada, H. Nambu, S. Hashimoto, *Chem. Eur. J.* **2011,** *17* (50), 13992-13998.

[12] a) K. M. Chepiga, Y. Feng, N. A. Brunelli, C. W. Jones, H. M. L. Davies, *Org. Lett.* **2013,** *15* (24), 6136-6139; b) E. G. Moschetta, S. Negretti, K. M. Chepiga, N. A. Brunelli, Y. Lebreche, Y. Feng, F. Rezaei, R. P. Lively, W. J. Koros, H. M. L. Davies, C. W. Jones, *Angew. Chem. Int. Ed.* **2015,** *54* (22), 6470-6474.

[13] a) K. Liao, S. Negretti, D. G. Musaev, J. Bacsa, H. M. L. Davies, *Nature* **2016,** *533* (7602), 230-234; b) K. Liao, T. C. Pickel, V. Boyarskikh, J. Bacsa, D. G. Musaev, H. M. L. Davies, *Nature* **2017,** *551* (7682), 609-613; c) K. Liao, Y. F. Yang, Y. Li, J. N. Sanders, K. N. Houk, D. G. Musaev, H. M. L. Davies, *Nat. Chem.* **2018,** *10* (10), 1048-1055; d) K. Liao, W. Liu, Z. L. Niemeyer, Z. Ren, J. Bacsa, D. G. Musaev, M. S. Sigman, H. M. L. Davies, *ACS Catal.* **2017,** *8* (1), 678-682; e) W. Liu, Z. Ren, A. T. Bosse, K. Liao, E. L. Goldstein, J. Bacsa, D. G. Musaev, B. M. Stoltz, H. M. L. Davies, *J. Am. Chem. Soc.* **2018,** *140* (38), 12247-12255.

[14] a) C. Qin, V. Boyarskikh, J. H. Hansen, K. I. Hardcastle, D. G. Musaev, H. M. L. Davies, *J. Am. Chem. Soc.* **2011,** *133* (47), 19198-19204; b) C. Qin, H. M. L. Davies, *J. Am. Chem. Soc.* **2014,** *136* (27), 9792-6.

[15] D. Zhao, J. Sun, Q. Li, G. D. Stucky, *Chem. Mater.* **2000,** *12*, 275-279.

[16] B. Wei, J. C. Sharland, P. Lin, S. M. Wilkerson-Hill, F. A. Fullilove, S. McKinnon, D. G. Blackmond, H. M. L. Davies, *ACS. Catal.* **2019,** *10* (2), 1161-1170.

[17] a) K. Tanabe, W. F. Hoelderich, *Appl. Catal. A-Gen.*, **1999**, *181*, 399-434; b) T. B. Lin, D. L. Chung, J. R. Chang, *Ind. Eng. Chem. Res.*, **1999**, *38*(4), 1271–1276; c) A. Sakthivel, S. K. Badamali, P. Selvam, *Micropor. Mesopor. Mat.,* **2000**, *39*, 457-463; d) B. Li, R. Yan, L. Wang, Y. Diao, Z. Li, S. Zhang, *Ind. Eng. Chem. Res.,* **2014**, *53*(4), 1386–1394; e) Q. N. Wang, L. Shi, A. H. Lu, *ChemCatChem,* **2015**, *7*, 2846 –2852; f) Z. Li, A. W. Peters, V. Bernales, M.I A. Ortuño, N. M. Schweitzer, M. R. DeStefano, L. C. Gallington, A. E. Platero-Prats, K. W. Chapman, C. J. Cramer, L. Gagliardi, J. T. Hupp, O. K. Farha*, ACS Cent. Sci.,* **2017**, *3*, 31−38; g) J. M. Carceller, M. Mifsud, M. J. Climent, S. Iborra, A. Corma, *Green Chem.*, **2020**, *22*, 2767-2777.

[18] The TOF was determined with a 0.13 molar solution of the diazo compound with 0.05 mol.% catalyst and 5 equiv. of styrene. Moisture and excess styrene are known to retard the catalyst, and even higher TOF can be obtained with Rh_2(*S*-*o*-ClTPCP)$_4$ under more stringent dry conditions using only 2.3 equiv. of styrene. See ref 12 for details.

WILEY-VCH

Entry for the Table of Contents

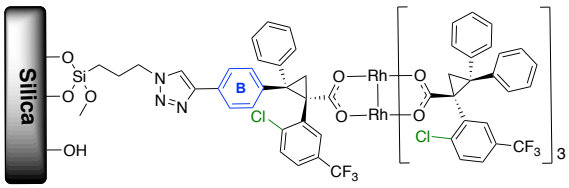

Supported Rh_2(*S*-2-Cl-5-CF_3TPCP)$_4$ catalysts ancored to mesoporous silica in three different locations demonstrates optimal tethering location, allowing for deployment in a fixed bed flow reactor for enanti- and regioselective C-H functionalization. Tuning silica particle size/shape enhances reactivity, with optimized catalyst enabling multiple catalysts recycles with comparable yields and selectivities to batch reactions. The catalyst immobilization methodology is widely applicable to a family of dirhodium carbene catalysts offering varying C-Hregioselectivity.

Institute and/or researcher Twitter usernames: @NSFCCHF; #NSFFunded

WILEY-VCH